

Designing Artificial Lieb Lattice on Metal Surface

Wen-Xuan Qiu,¹ Shuai Li,¹ Jin-Hua Gao,^{1,*} Yi Zhou,^{2,3} and Fu-Chun Zhang^{2,3}

¹*School of Physics and Wuhan National High Magnetic field center, Huazhong University of Science and Technology, Wuhan 430074, China*

²*Department of Physics, Zhejiang University, Hangzhou, China*

³*Collaborative Innovation Center of Advanced Microstructures, Nanjing 210093, China*

Recently, several experiments^{1,2} have illustrated that metal surface electrons can be manipulated to form a two dimensional (2D) lattice by depositing a designer molecule lattice on metal surface. This offers a promising new technique to construct artificial 2D electron lattices. Here we theoretically propose a molecule lattice pattern to realize an artificial Lieb lattice on metal surface, which shows a flat electronic band due to the lattice geometry. We show that the localization of electrons in the flat band may be understood from the viewpoint of electron interference, which may be probed by measuring the local density of states with the scanning tunnelling microscopy. Our proposal may be readily implemented in experiment and may offer an ideal solid state platform to investigate the novel flat band physics of the Lieb lattice.

The two-dimensional (2D) lattices with flat electron bands are of special research interests³⁻⁵. The electrons in such flat bands are localized due to the destructive wave interference resulted from the special lattice geometries. By the flat band, we mean the kinetic energy of electrons to be quenched, so that tiny interactions can induce various exotic many-body states, such as ferromagnetism^{3,6}, Wigner crystal⁷ and superconductivity⁸⁻¹⁰. More recently, it has been pointed out that if nontrivial topology can be introduced into flat band, fractional quantum Hall states may occur in the absence of an external magnetic field¹¹⁻¹⁵. Due to these novel properties, great efforts have been made in the recent years to search 2D flat band systems in real materials¹⁶ as well as in artificial 2D lattice systems such as cold atom¹⁷⁻¹⁹, photonic crystal^{20,21}, quantum dot lattice²² and circuit QED lattice²³.

The Lieb lattice is one of the most well-known 2D flat band lattices. It is a line centered square lattice, and is composed of three atoms (A,B,C) in one unit cell (see in Fig. 1). The dispersion of the tight-binding model with nearest neighbor hopping on the Lieb lattice consists of three bands including a flat band in the middle of the spectra. At half filling, infinitesimal on-site Coulomb interaction can induce a ferromagnetic ground state, i.e. the flat band ferromagnetism⁶. More interestingly, away from the half filled, the spin-orbit coupling can induce various exotic topologically nontrivial phases in the Lieb lattice²⁴⁻²⁶. Under certain conditions, the flat band of the Lieb lattice may have a nonzero Chern number, which is crucial to realize fractional Chern insulator^{27,28}. Recently, it is reported that the Lieb lattice has been realized in photonic crystal^{20,21} and cold atom system²⁹. However, searching the Lieb lattice of electrons in a solid state system remains a challenge and is badly needed for the intriguing theoretical proposals.

In this work, we propose a practical scheme to induce a tunable artificial Lieb lattice on metal surface. The basic idea is motivated by a recent experiment where an artificial graphene is successfully realized on metal surface^{1,2}. In that experiment, CO molecules are assem-

bled on Cu(111) surface by scanning probe technique to form a hexagonal lattice, in which each CO molecule becomes a repulsive potential center on the metal surface and the surface electrons are effectively confined on the discrete sites of an artificial honeycomb lattice and have a linear dispersion^{1,30,31}. Here we theoretically propose a special arrangement of the CO molecules and show that the metal surface electrons can be transformed into a Lieb lattice with a flat or nearly flat band. We first use numerical method to find the electronic band structure of the metal surface electrons when the proposed CO molecules are absorbed, followed by a tight binding model fitting with nearest neighbor (NN) and next nearest neighbor (NNN) hopping integrals on the Lieb lattice. Due to a small but finite NNN hopping, the flat band on this artificial Lieb lattice is bended with a narrow band width and a large DOS, and small interactions may lead to instabilities of the long range ordered states. The flatness of the flat band electrons on this artificial Lieb lattice depends on the strength of the repulsive potential applied by the absorbed molecule. The larger the repulsive potential is, the flatter the band is. Meanwhile, the filling number of electrons on the Lieb lattice is also controllable. An interesting issue is the wave function localization of the flat band electrons. Due to the geometric phase cancellation, the flat band electrons of the Lieb lattice are localized only at the B and C sites, which gives a unique LDOS pattern for the flat band electrons. This special type of LDOS is demonstrated in our numerical simulation, which can be directly probed in the scanning tunnelling microscopy (STM).

Our proposal is of several merits: (1) it is a solid state electronic system, and has intrinsic Coulomb interaction which is essential for these exotic many-body states of flat band fermions; (2) because that the artificial Lieb lattice is made on the metal surface, we may apply various techniques available in condensed matter physics to detect the electronic structure of the flat band, e.g. the STM to detect the LDOS, possible charge order (or spin order), and even the edge states which is crucial for the topological nontrivial phases. (3) It should be accessi-

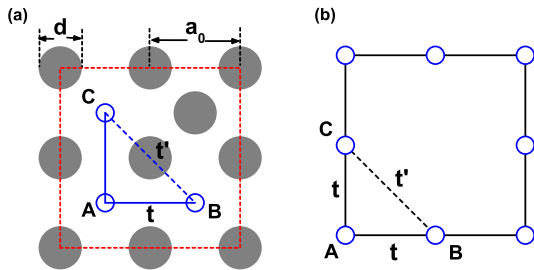


FIG. 1. (Color online) (a) The muffin-tin potential proposed in this paper to induce artificial Lieb lattice with nearly flat electron band. In the model calculation, the potential is U_0 inside the gray dots which represent the absorbed molecules and zero outside the dots. d is the diameter of the potential dots and a_0 is the lattice constant of the molecule lattice. The red dashed lines indicate the unit cell of the 2D system in the presence of the muffin-tin potential. The blue circles represent the three sites (A, B, C) in a unit cell of the artificial Lieb lattice for the surface electrons. t and t' are the NN and NNN hopping integrals, respectively. (b) The equivalent Lieb lattice.

ble to implement this scheme in experiment since that the same technique has been used to realize an artificial honeycomb lattice (molecule graphene).

In order to make our proposal more realistic, we consider the system of Cu(111) surface and CO molecules which was used to construct the molecule graphene. The Cu surface state can be viewed as a 2D electron gas (2DEG) with parabolic dispersion, and the Hamiltonian is $H_{\text{Cu}} = \frac{\hbar^2 k^2}{2m^*}$, where $m^* = 0.38m_e$ is the effective mass. The Fermi energy is $E_f = 0.45$ eV from the band bottom. When a CO molecule is absorbed on the Cu surface, it exerts a repulsive potential on the underlying surface electrons. Thus, if the CO molecules are assembled into a lattice on metal surface, the surface electrons feel a lateral periodic potential and can be forced into a fermionic lattice system. Note that, this Cu/CO system is a quantum antidot system since the CO molecule will deplete the underlying surface electrons. In theory, the potential of the CO molecule lattice can be approximated as a muffin-tin potential $U(r)$. We can obtain the energy dispersion of the modified Cu surface states via solving the system Hamiltonian $H = H_{\text{Cu}} + U(r)$ by plane wave method^{30,32}.

The muffin-tin potential we propose to induce an artificial electron system on a Lieb lattice is illustrated in Fig. 1 (a). U_0 (> 0) inside the gray dots and zero elsewhere. Here a gray dot represents a CO molecule or the potential of CO molecule. Note that a Lieb lattice can be achieved via removing one quarter of the sites of the square lattice (see Fig. 1(b)). Following this basic idea, we first arrange the CO molecules into a square lattice, where lattice constant is a_0 as shown in Fig. 1 (a). Consequently, due to

the repulsive periodic potential of the CO molecule lattice, the metal surface electrons are forced also into a square lattice with the same lattice constant, where the lattice sites (blue circles) are at the center of the squares formed by four neighbouring molecules. Then, we delete one of the four sites of surface electron lattice by positioning an additional molecule to the center of the upper right square, as shown in Fig. 1(a). Finally, we get an artificial Lieb lattice of surface electrons in such antidot lattice system. The red dotted line in Fig. 1 (a) gives the unit cell of the muffin-tin potential, and the corresponding Lieb lattice of the surface electrons is shown in Fig. 1 (b). We use t and t' to denote the NN and NNN hopping integrals, respectively.

Now, we show that the low energy physics of the artificial 2D system is equivalent to electrons on a Lieb lattice. We first calculate the energy dispersion of the surface electrons in the presence of the molecules by the plane wave method, and then we show that the three lowest mini-bands, induced by the lateral periodic potential, can be well described by the tight binding model of the Lieb lattice.

Let us first discuss the calculation of energy dispersion. With the plane wave method, there are three parameters of the muffin-tin potential in our model: the lattice constant a_0 , the potential value U_0 and the potential diameter d (see in Fig. 1). Here, a_0 is the distance between adjacent molecules, which is tunable in experiment. $U_0 = 7$ eV and $d = 0.5$ nm are the reasonable values of Cu/CO system got by fitting the experiments³⁰.

Meanwhile, the tight binding Hamiltonian of the Lieb lattice is

$$H = - \sum_{ij,\sigma} t_{ij} c_{i\sigma}^+ c_{j\sigma} + \sum_{i\sigma} \epsilon_i c_{i\sigma}^+ c_{i\sigma}, \quad (1)$$

where $c_{i\sigma}^+$ creates an electron with spin σ on lattice site i . The unit cell of the Lieb lattice is given by A, B, C sites shown in Fig. 1, and we consider the NN hopping t and NNN hopping t' . For square lattice, there is an approximate relation about the NN hopping t with the underlying 2D system,

$$t = \frac{\hbar^2}{2m^* a_0^2}, \quad (2)$$

which we will choose for the Lieb lattice model with an additional fitting parameter of the NNN hopping t' . Note that the circumstance of the B (and C) site is different from that of A site in Fig. 1 (a), so that in the tight binding model the onsite energy of B and C sites are equal, but can be different from that of A site. The Hamiltonian is a 3×3 matrix

$$H(k) = \begin{pmatrix} \epsilon_A & -2t \cos(k_x a_0) & -2t \cos(k_y a_0) \\ -2t \cos(k_x a_0) & \epsilon_B & -4t' \cos(k_x a_0) \cos(k_y a_0) \\ -2t \cos(k_y a_0) & -4t' \cos(k_x a_0) \cos(k_y a_0) & \epsilon_C \end{pmatrix} \quad (3)$$

We set $\epsilon_B = \epsilon_C = \epsilon_0 + \Delta$ and $\epsilon_A = \epsilon_0 - \Delta$, where ϵ_0 and Δ are parameters to be determined. When $t' = 0$, the dispersion of the tight binding model is simple, and it gives two dispersive bands $\epsilon_{\pm}(k) = \epsilon_0 \pm \sqrt{4t^2[\cos^2(k_x a_0) + \cos^2(k_y a_0)] + \Delta^2}$ and one dispersionless flat band $\epsilon(k) = \epsilon_0 + \Delta$. It should be noted that, when $\Delta = 0$, i.e. $\epsilon_A = \epsilon_B = \epsilon_C$, the three bands touch at the M point in the FBZ, while if $\Delta \neq 0$, the flat band touch only one dispersive band at M point and a gap about $2|\Delta|$ can be observed at M point. In addition, it can be seen from the TB model that the wave function of the flat band electrons of Lieb lattice only locates at B and C sites. If t' is nonzero, the analytical expressions of the energy dispersion become more complex and numerical calculation may be a better way. However, the properties above approximately hold when t' is not too large.

The numerical results of the energy bands are shown in Fig. 2. In Fig. 2 (a), we plot the lowest three bands of the calculated band structure got by the plane wave method, with the lattice constant $a_0 = 9.5 \text{ \AA}$ (blue solid lines). Meanwhile, the tight binding bands of the Lieb lattice are given as a comparison (red dashed lines), with a t got by Eq. 2 and a fitted t' . We see that, the three plane wave bands, especially the lowest two, can be well described by the tight binding model of Lieb lattice. Note that here, once a_0 is given, the NN hopping t is fixed and t' is got by fitting the band shape, while ϵ_0 and Δ are got by fitting the energy gap at M point. One important characteristic is that, due to the nonzero t' , the middle band of the Lieb lattice is not completely flat but bended. However, it still has a narrow band width and a giant DOS as given in Fig. 2 (b), which is much larger than that near Van Hove singularities. In addition, because that the onsite energy of B (and C) site is different from that of A site, i.e. $\Delta \neq 0$, the flat band only touches the upper band at M point in FBZ, and has a small gap about $2|\Delta| \approx 24 \text{ meV}$ at M point from the lower band. Note that, since that the middle band is bended away from the M point, this small gap can not be observed from the DOS. This is an intrinsic property of this artificial Lieb lattice. We then plot the calculated bands in the whole FBZ in Fig. 3 (a). All the characteristics mentioned above are also shown clearly.

In this artificial Lieb lattice, the flatness of the flat band is tunable. Actually, the flatness of the middle band of Lieb lattice depends on the NNN hopping t' . Smaller t' gives a flatter band. In this artificial Lieb lattice, t' is determined by the value of muffin-tin potential U_0 . This point can be understood from Fig. 1 (a). We see that t' is the hopping between B and C sites, which is blocked by an in-between molecule. Intuitively, the stronger the

potential U_0 is the smaller t' is, and thus a flatter band can be achieved. This understanding is confirmed by the numerical results with a larger value of U_0 , which are plotted in Fig. 2 (c), (d) and Fig. 3 (b). With $U_0 = 7 \text{ eV}$ in Fig. 2 (a), the band width of the middle band is

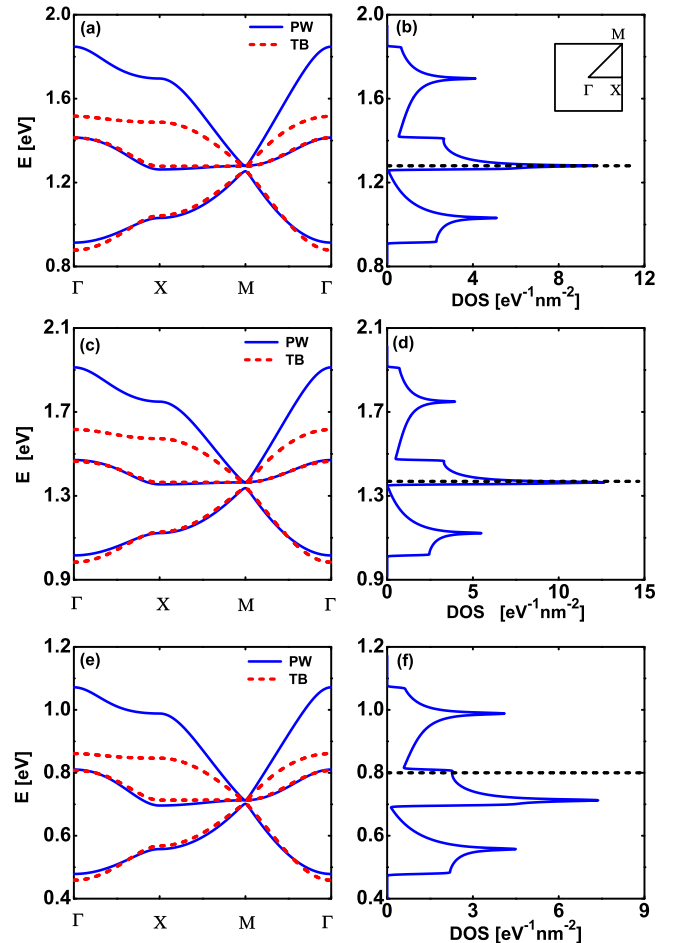


FIG. 2. (Color online) Left panels: three lowest bands (blue lines) calculated within plane wave (PW) method for the muffin-tin potential given in Fig. 1 and the fitting electron bands (red dotted lines) within the tight-binding (TB) model of the Lieb lattice in Eq. (1) for 3 sets of the parameters in Fig. 1 (a). $U_0 = 7 \text{ eV}$, $a_0 = 0.95 \text{ nm}$ and $d = 0.5 \text{ nm}$. The fitting parameters in TB are $t = 0.11 \text{ eV}$, $t' = 0.034 \text{ eV}$, $\Delta = 0.012 \text{ eV}$ and $\epsilon_0 = 1.27 \text{ eV}$. (c) $U_0 = 9 \text{ eV}$, $a_0 = 0.95 \text{ nm}$ and $d = 0.5 \text{ nm}$. The fitting parameters in Eq. (1) are $t = 0.11 \text{ eV}$, $t' = 0.025 \text{ eV}$, $\Delta = 0.014 \text{ eV}$ and $\epsilon_0 = 1.35 \text{ eV}$. (e) $U_0 = 7 \text{ eV}$, $a_0 = 1.2 \text{ nm}$ and $d = 0.5 \text{ nm}$. The fitting parameters in Eq. (1) are $t = 0.069 \text{ eV}$, $t' = 0.023 \text{ eV}$, $\Delta = 0.006 \text{ eV}$ and $\epsilon_0 = 0.71 \text{ eV}$. Right panel: (b),(d), (f) are the corresponding DOS for the cases of (a), (c),(e), respectively. The black dotted line is the Fermi level.

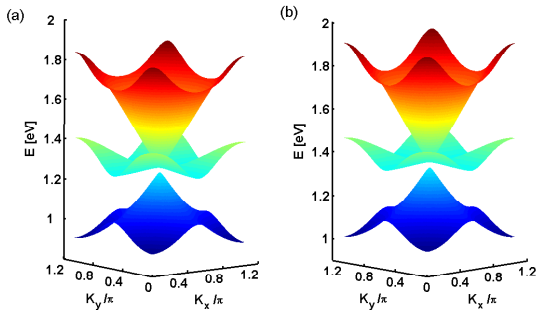


FIG. 3. (Color online) The lowest three energy bands calculated by plane wave method in the FBZ. (a) is for the case of Fig. 2 (a). (b) is for the case of Fig. 2 (c).

about 150 meV, while with $U_0 = 9$ eV it becomes 120 meV in Fig. 2 (c). So, a flatter band can be achieved by choosing a proper molecule with stronger repulsive potential.

Meanwhile, the position of the Fermi level is also controllable in this system by tuning the lattice constant a_0 . Note that, in order to investigate the physics of flat band, the Fermi level should be in or close to the flat band. Or equivalently, the filling of Lieb lattice should be in the region between $\frac{1}{3}$ and $\frac{2}{3}$. An assumption here is that the total electron number of the metal surface states is fixed even in the presence of the absorbed molecules. Therefore, with different a_0 , the band structure is different and thus the position of Fermi level is changed accordingly. We now give some quantitative estimations. The filling of this artificial Lieb lattice is $\frac{2}{3}N_e a_0^2$, where N_e is the electron density of the metal surface. For Cu(111) surface, to access the flat band, a_0 should be in the region $0.8 \text{ nm} < a_0 < 1.2 \text{ nm}$, where N_e is about 0.72 nm^{-2} . For half filling which has an exact ferromagnetic ground state, a_0 is about 1.0 nm. For larger a_0 , the Fermi level is at the upper band, as shown in Fig. 2 (e) and (f). These estimations are general for the Cu(111) surface no matter which kind of molecule is used in experiment. We emphasize that the required region of a_0 above has already been achieved in the molecule graphene experiments^{1,2}.

The second illustration for the Lieb lattice is the special LDOS pattern of the flat band electrons. As described above, one intriguing property of the flat band of Lieb lattice is that the wave function is localized on the B and C sublattices, and vanish on the A sublattice. We reveal this property by calculating the LDOS of surface electron

$$\text{LDOS}(r, \epsilon) = \sum_{nk\sigma} |\Phi_{nk\sigma}(r)|^2 \delta(\epsilon - \epsilon_{nk}) \quad (4)$$

which can be directly measured by the STM. From the definition of the LDOS, it is easy to see that, if it is a Lieb lattice, the LDOS of the flat band electrons should have finite values around the B and C sublattices and be zero around the A sublattice. In Fig. 4, we plot the LDOS of the artificial Lieb lattice with different energy, where the corresponding bands are given in Fig. 2 (c). In

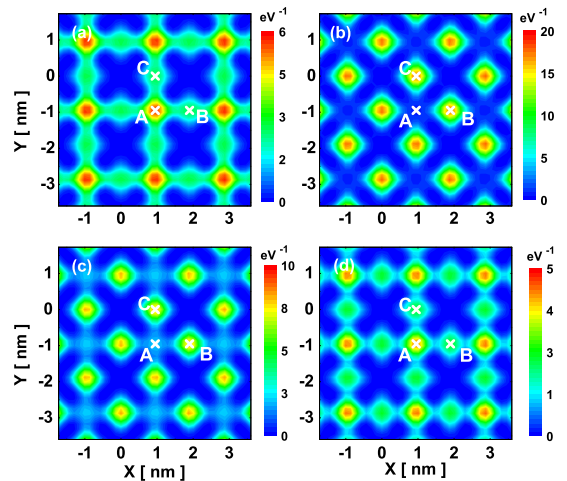


FIG. 4. (Color online) The LDOS pattern in real space with different energy. The potential parameters are the same as that used in Fig. 2 (c). (a) $\epsilon = 1.2$ eV. (b) $\epsilon = 1.37$ eV. (c) $\epsilon = 1.5$ eV. (d) $\epsilon = 1.6$ eV

Fig. 4 (a), $\epsilon = 1.2$ eV and thus the electrons are from the lower band. We see that electron distribution is nonzero around all the three sites, but the amplitude around the A site is much larger than that around the B (and C) site. This is consistent with the TB results. The LDOS with $\epsilon = 1.37$ eV is given in Fig. 4 (b), where the electrons mainly are from the middle band (flat band). Obviously, the LDOS becomes nearly zero around A sublattice and is finite around B and C sublattices. That is just the wave function localization phenomenon of Lieb lattice. If slightly increasing the energy, at $\epsilon = 1.5$ eV, there are electrons from both the middle band and upper band. Now the electron distribution at A site becomes nonzero but tiny, while the electrons are still mainly distributed at B and C sites (see in Fig. 4 (c)). It implies that in this case the electrons from the flat band dominate. Increasing the energy further, we plot the LDOS pattern with $\epsilon = 1.6$ eV in Fig. 4 (d), where the electrons are only from the upper band. The case is the similar as that of lower band. So, in the STM experiment, the LDOS for different energy (i.e. different bias voltage) can give an direct evidence of the wave function localization of flat band electrons, and thus can be used to identify the flat band states as well as the Lieb lattice. We would like to emphasize that, in this system, the wave function localization of flat band is an interference phenomenon of the surface electrons in the presence of a special absorbed molecule lattice. In fact, the absorbed molecule (or atom) induced interference phenomena are usual on metal surface, e.g. standing wave of surface electron and the celebrated quantum corral. Thus, it should not be surprising that this wave function localization can be observed in experiment.

In summary, we theoretically propose a scheme to realize an artificial Lieb lattice on the metal surface via

the technique reported in the recent molecule graphene experiments. All the requirements of this scheme have already been fulfilled in the recent molecule graphene experiments, so that it can be easily implemented in experiment. Considering that the external magnetic field, as well as the spin-orbit coupling, can be readily induced, we think that this artificial Lieb lattice on metal surface is an ideal solid state platform to study the novel flat band physics of Lieb lattice, e.g. the wave function localization of the flat band electrons, the correlated states and the possible topological nontrivial phases. We point

out that the LDOS measured by STM can be used to identify the wave function localization of the flat band electrons.

This work is supported by the National Science Foundation of China (Grants No. 11274129, No. 11534001, No.11374256/11274269/11674278), National Basic Research Program of China (No.2014CB921201/2014CB921203) and National Key R&D Program of the MOST of China (No.2016YFA0300202),. F.C.Z was also supported by the Hong Kong University Grant Council via Grant No. AoE/P-04/08.

* jinhua@hust.edu.cn

- ¹ K. K. Gomes, W. Mar, W. Ko, F. Guinea, and H. C. Manoharan, *Nature* **483**, 306 (2012).
- ² S. Wang, L. Z. Tan, W. Wang, S. G. Louie, and N. Lin, *Phys. Rev. Lett.* **113**, 196803 (2014).
- ³ H. Tasaki, *Prog. Theor. Phys.* **99**, 489 (1998).
- ⁴ Z. Liu, F. Liu, and Y.-S. Wu, *Chin. Phys. B.* **23**, 077308 (2014).
- ⁵ E. J. Bergholtz and Z. Liu, *Int. J. Mod. Phys. B* **27**, 1330017 (2013).
- ⁶ E. H. Lieb, *Phys. Rev. Lett.* **62**, 1201 (1989); A. Mielke, *J. Phys. A: Math. Gen.* **24**, L73 (1991); S.-Q. Shen, Z.-M. Qiu, and G.-S. Tian, *Phys. Rev. Lett.* **72**, 1280 (1994).
- ⁷ C. Wu, D. Bergman, L. Balents, and S. Das Sarma, *Phys. Rev. Lett.* **99**, 070401 (2007).
- ⁸ S. Miyahara, S. Kusuta, and N. Furukawa, *Physica C* **460**, 1145 (2007).
- ⁹ A. Julku, S. Peotta, T. Vanhala, D.-H. Kim, and P. Törmä, arXiv:1603.03237 [cond-mat] (2016).
- ¹⁰ N. B. Kopnin, T. T. Heikkilä, and G. E. Volovik, *Phys. Rev. B* **83**, 220503 (2011).
- ¹¹ E. Tang, J.-W. Mei, and X.-G. Wen, *Phys. Rev. Lett.* **106**, 236802 (2011).
- ¹² T. Neupert, L. Santos, C. Chamon, and C. Mudry, *Phys. Rev. Lett.* **106**, 236804 (2011).
- ¹³ K. Sun, Z. Gu, H. Katsura, and S. Das Sarma, *Phys. Rev. Lett.* **106**, 236803 (2011).
- ¹⁴ D. N. Sheng, Z.-C. Gu, K. Sun, and L. Sheng, *Nat. Commun.* **2**, 389 (2011).
- ¹⁵ N. Regnault and B. A. Bernevig, *Phys. Rev. X* **1**, 021014 (2011).
- ¹⁶ Z. Liu, Z.-F. Wang, J.-W. Mei, Y.-S. Wu, and F. Liu, *Phys. Rev. Lett.* **110**, 106804 (2013).
- ¹⁷ R. Shen, L. B. Shao, B. Wang, and D. Y. Xing, *Phys. Rev. B* **81**, 041410 (2010).
- ¹⁸ N. Goldman, D. F. Urban, and D. Bercioux, *Phys. Rev. A* **83**, 063601 (2011).
- ¹⁹ V. Apaja, M. Hyrkäs, and M. Manninen, *Phys. Rev. A* **82**, 041402 (2010).
- ²⁰ R. A. Vicencio, C. Cantillano, L. Morales-Inostroza, B. Real, C. Mejía-Cortés, S. Weimann, A. Szameit, and M. I. Molina, *Phys. Rev. Lett.* **114**, 245503 (2015).
- ²¹ S. Mukherjee, A. Spracklen, D. Choudhury, N. Goldman, P. Öhberg, E. Andersson, and R. R. Thomson, *Phys. Rev. Lett.* **114**, 245504 (2015).
- ²² H. Tamura, K. Shiraishi, T. Kimura, and H. Takayanagi, *Phys. Rev. B* **65**, 085324 (2002).
- ²³ Z.-H. Yang, Y.-P. Wang, Z.-Y. Xue, W.-L. Yang, Y. Hu, J.-H. Gao, and Y. Wu, *Phys. Rev. A* **93**, 062319 (2016).
- ²⁴ C. Weeks and M. Franz, *Phys. Rev. B* **82**, 085310 (2010).
- ²⁵ A. Zhao and S.-Q. Shen, *Phys. Rev. B* **85**, 085209 (2012).
- ²⁶ W.-F. Tsai, C. Fang, H. Yao, and J. Hu, *New J. Phys.* **17**, 055016 (2015).
- ²⁷ B. Jaworowski, A. Manolescu, and P. Potasz, *Phys. Rev. B* **92**, 245119 (2015).
- ²⁸ I. N. Karnaukhov and I. O. Slieptsov, arXiv:1510.07239 [cond-mat] (2015); arXiv:1604.05039 [cond-mat] (2016).
- ²⁹ S. Taie, H. Ozawa, T. Ichinose, T. Nishio, S. Nakajima, and Y. Takahashi, *Sci. Adv.* **1**, e1500854 (2015).
- ³⁰ S. Li, W.-X. Qiu, and J.-H. Gao, *Nanoscale* **8**, 12747 (2016).
- ³¹ M. Ropo, S. Paavilainen, J. Akola, and E. Räsänen, *Phys. Rev. B* **90**, 241401 (2014).
- ³² C.-H. Park and S. G. Louie, *Nano Lett.* **9**, 1793 (2009).